



**HAL**  
open science

## Investigation of weather anomalies in the low-latitude islands of the Indian Ocean in 1991

Anne Réchou, S. Kirkwood

► **To cite this version:**

Anne Réchou, S. Kirkwood. Investigation of weather anomalies in the low-latitude islands of the Indian Ocean in 1991. *Annales Geophysicae*, 2015, 33, pp.789-804. 10.5194/angeo-33-789-2015 . hal-01173951

**HAL Id: hal-01173951**

**<https://hal.science/hal-01173951v1>**

Submitted on 21 Oct 2016

**HAL** is a multi-disciplinary open access archive for the deposit and dissemination of scientific research documents, whether they are published or not. The documents may come from teaching and research institutions in France or abroad, or from public or private research centers.

L'archive ouverte pluridisciplinaire **HAL**, est destinée au dépôt et à la diffusion de documents scientifiques de niveau recherche, publiés ou non, émanant des établissements d'enseignement et de recherche français ou étrangers, des laboratoires publics ou privés.



# Investigation of weather anomalies in the low-latitude islands of the Indian Ocean in 1991

A. Réchou<sup>1</sup> and S. Kirkwood<sup>2</sup>

<sup>1</sup>Laboratoire de l'Atmosphère et des Cyclones, UMR8105, CNRS, Météo-France, Université de La Réunion, Réunion, France

<sup>2</sup>Swedish Institute of Space Physics, Box 812, 981 28 Kiruna, Sweden

Correspondence to: A. Réchou (arechou@univ-reunion.fr)

Received: 15 November 2014 – Revised: 13 April 2015 – Accepted: 10 June 2015 – Published: 02 July 2015

**Abstract.** Temperature, precipitation and sunshine duration measurements at meteorological stations across the southern Indian Ocean have been analysed to try to differentiate the possible influence of the Mount Pinatubo volcanic eruption in the Philippines in June 1991 and the normal weather forcings. During December 1991, precipitation on the tropical islands Glorieuses (11.6° S) and Mayotte (12.8° S) was 4 and 3 times greater, respectively, than the climatological mean (precipitation is greater by more than twice the standard deviation (SD)). Mean sunshine duration (expressed in sun hours per day) was only 6 h on Mayotte, although the sunshine duration is usually more than  $7.5 \pm 0.75$  h, and on the Glorieuses it was only 5 h, although it is usually  $8.5 \pm 1$  h. Mean and SD of sunshine duration are based on December (1964–2001 for Mayotte, 1966–1999 for the Glorieuses).

The Madden–Julian Oscillation (MJO) is shown to correlate best with precipitation in this area. Variability controlling the warm zone on these two islands can be increased by the Indian Ocean Dipole (IOD), El Niño, the quasi-biennial oscillation (QBO) and/or solar activity (sunspot number, SSN). However, temperature records of these two islands show weak dependence on such forcings (temperatures are close to the climatological mean for December). This suggests that such weather forcings have an indirect effect on the precipitation.

December 1991 was associated with unusually low values of the MJO index, which favours high rainfall, as well as with El Niño, eastern QBO and high SSN, which favour high variability. It is therefore not clear whether the Mount Pinatubo volcanic eruption had an effect. Since the precipitation anomalies at the Glorieuses and Mayotte are more or less local (Global Precipitation Climatology Project (GPCP) data) and the effect of the Pinatubo volcanic cloud

should be more widespread, it seems unlikely that Pinatubo was the cause.

Islands at higher southern latitudes (south of Tromelin at 15.5° S) were not affected by the Pinatubo eruption in terms of sunshine duration, precipitation or temperature.

**Keywords.** Meteorology and atmospheric dynamics (precipitation)

## 1 Introduction

Although it is well established that anthropogenic climate change is taking place on a global scale, the quantification and prediction at the regional scale is still very uncertain. In practice, small changes in the atmospheric circulation strongly affect regional climate (Shepherd, 2014). For example, planetary waves provide non-local teleconnections between El Niño–Southern Oscillation (ENSO) and the Indian Ocean monsoon. Moreover, since precipitation depends on both temperature and circulation, precipitation prediction is the most uncertain of all.

In this paper, unusually intense precipitation and other meteorological anomalies are reported which occurred over the Indian Ocean during the few months following June 1991. In that year, many different mechanisms could have been responsible for such anomalies, including the major volcanic eruption of Mount Pinatubo, which occurred in June 1991.

Many studies have been done to try to identify the mechanisms by which the Mount Pinatubo eruption and/or the weather forcing could modify regional climate. Often, large and explosive volcanic eruptions inject water vapour, carbon dioxide, sulfur dioxide, hydrogen chloride, hydrogen fluoride and ashes into the troposphere. These can reach the strato-

sphere (up to 20–30 km above the Earth's surface) mainly when eruptions occur in the tropical band, where vertical convective motions are large and help to increase the ascent rate of the air. Sulfur dioxide is converted into sulfuric acid, which condenses rapidly in the stratosphere to form sulfate aerosols. These particles are trapped in the lower stratosphere and circulate horizontally on the isentropes over the tropics for several consecutive months and then spread to higher latitudes before finally slowly sedimenting down to the ground. These stratospheric aerosols have a large radiative impact, affecting all heights down to the surface (Jones et al., 2003; Robock and Mao, 1995), and could probably induce many changes in the weather patterns, leading to large societal or economic consequences. For instance, the Russian famine of 1601–1603 was believed to have been caused by the Huaynaputina eruption of 1600 in South America (Verosub and Lippman, 2008).

In this case, the eruption of Mount Pinatubo (15.1° N, 121.4° E) on 15 June 1991 was the largest during the last 100 years and injected 14 to 20 Mt of SO<sub>2</sub> into the stratosphere (Bluth et al., 1992). The injected SO<sub>2</sub> was chemically transformed to sulfate aerosols which encircled the globe within a month (McCormick and Veiga, 1992). Although some aerosol loading from preceding volcanic eruptions (e.g. from El Chichón) was confined to the Northern Hemisphere, aerosols from the Mount Pinatubo eruption crossed the Equator (Michalsky et al., 1994). McCormick and Veiga (1992) used SAGE II observations prior to and after June 1991 and showed that the optical thickness of the aerosol cloud doubled between 10° S and 30° N soon after the Pinatubo eruption (15 June–25 July 1991). In June, July and early August, the top of the aerosol cloud in the tropics reached up to 29 km altitude (although it was mostly between 20 and 25 km altitude). Because of the small size of aerosols, the reflection of shortwave solar radiation is higher than the attenuation of the longer-wavelength Earth-emitted radiation.

Dutton and Christy (1992) reported a reduction in the direct visible radiation reaching the ground and a concomitant increased backscattering to space as a result of this Mount Pinatubo eruption. Changes in radiative forcing due to these processes influenced the land temperatures in the second and third summers following tropical eruptions (Jones et al., 2003) and may influence the vertical and meridional temperature gradients and induce modifications of the larger-scale circulation as discussed by Hofmann (1987).

Church et al. (2005) found a reduction in ocean heat content of about  $3 \times 10^{22}$  J and a global sea level fall of about 5 mm. Over the 3 years following the Pinatubo eruption, they estimated a decrease in evaporation of up to 0.1 mm day<sup>-1</sup>. A lowering of air temperatures was observed after the Pinatubo eruption and a reduced total water vapour in the atmosphere (Trenberth and Smith, 2005; Soden et al., 2005). In fact, changes in radiative forcing directly perturb the thermodynamic balance of the climatic system, and the response is

a change in atmospheric temperature as well as associated quantities such as humidity.

Precipitation and hydrological effects are more difficult to analyse and model (Broccoli et al., 2003). Trenberth and Dai (2007), examining precipitation from 1950 to 2004 on a global scale, show a substantial decrease over land and an exceptional decrease in runoff and river discharge from October 1991 to September 1992.

As described by Trenberth and Dai (2007), the Pinatubo eruption took place during ENSO, which itself causes substantial re-organization of the circulation in the southern tropics and so brings more rain in some places than in others. For example, Curtis and Adler (2003), using 23-year (1979–2001) satellite-gauge estimates, found that, during El Niño events, there was a decrease in precipitation over land but an increase over the ocean.

Before the eruption, ENSO had already been in its positive phase since 1990. Nevertheless, it remained in this phase for an extremely long time after 1990 (the next La Niña (negative phase) occurred in 1996).

ENSO presents a warm phase in March–April (seasonal minimum in the strength of equatorial easterlies) and a cold phase reaching its maximum in September–October. The mechanism through which ENSO exerts its influence on the Indian Ocean is not clearly understood, but it has been related to the changes in zonal Walker circulation and thus affects the weather in all ocean basins (e.g. including the Indian Ocean).

Added to this situation, the positive phase of the Indian Oscillation Dipole (IOD) may have an influence on weather events, in particular precipitation in the Indian Ocean. In fact, the IOD is a mode of variability in sea surface temperature (SST) that seriously affects the climate around the Indian Ocean (Saji et al., 1999; Morioka et al., 2010). A positive IOD period is characterized by cooler than normal water in the tropical eastern Indian Ocean and warmer than normal water in the tropical western Indian Ocean. Positive IOD often develops in May/June, peaks in September/October and diminishes in December/January. The anomalous SSTs are found to be closely correlated with changes in surface winds. For example, the equatorial winds reverse direction from westerlies to easterlies during the peak phase of the positive phase IOD events (i.e. SST is cool in the east and warm in the west; see Chang et al., 2005). The atmospheric component of IOD is seen in OLR (outgoing longwave radiation) anomalies (Behera et al., 1999, 2003; Yamagata et al., 2002) and sea level pressure anomalies (Behera and Yamagata, 2003).

In this study, the influence of different geophysical climate forcings (such as IOD and ENSO), including the Pinatubo eruption, on precipitation and sunshine duration anomalies following June 1991.

Different theories exist about the influence of ENSO with or without IOD (pure ENSO) on the climate of the Indian Ocean. Positive IOD together with El Niño is accompanied by subsidence over the cold IOD pole and upward motion over the warm pole, as shown by the atmospheric general

circulation model (AGCM) experiment reported in Ashok et al. (2003, 2004). Yamagata et al. (2003) demonstrated that an anomalous Walker cell exists in the Indian Ocean but is visible only during pure IOD events (without ENSO). Pure IOD periods are associated with stronger SST anomalies (Yamagata et al., 2004). Additionally, it has been suggested that there is an influence of the IOD on the monsoon (Ashok et al., 2004). It has also been suggested that there is an unstable, coupled ocean–atmosphere mode enabling the IOD to be strong and independent in some years and forced more directly by ENSO in other years, particularly in the July–November season (Yuan and Li, 2008). From pure El Niño composites (without IOD), Chang et al. (2005) reported that cold SST anomalies of Pacific origin, entering the Indian Ocean, propagate along the west coast of Australia.

The Indian Ocean is also affected by the Madden–Julian Oscillation (MJO), which originates in the west of the Indian Ocean (Madden and Julian, 1971, 1994; Jones et al., 1998) and propagates eastward slowly at around  $5 \text{ m s}^{-1}$  (Elleman, 1997). This wave is the dominant, but not the only, component of the intraseasonal (30–90-day period) variability in the tropical atmosphere (from  $30^\circ \text{ N}$  to  $30^\circ \text{ S}$ ) (Lau and Waliser, 2005). Large-scale coupled patterns in atmospheric circulation and deep convection compose the MJO and interact with the ocean, influencing many weather and climate systems (Zhang, 2005). The MJO involves variation in wind, SST, cloudiness and rainfall.

In the stratosphere, the quasi-biennial oscillation (QBO) controls the zonal winds, although the QBO does not penetrate significantly below the tropopause (Baldwin et al., 2001). However in the tropics, there is a possibility that the tropopause is uplifted by strong convective activity and that the cloud tops reach altitudes of 16 km (Fueglistaler et al., 2009), where the influence of QBO winds is still felt. Thus, the cloud top can drift in the lower QBO winds, which can reach downward to near 16 km. Moreover, over the Indian Ocean region, Jury et al. (1994), analysing SST, OLR, QBO and tropospheric wind in relation to the Southern Oscillation Index (SOI), found an effect of the QBO on summer rainfall. A dipole was found during the west phase of the QBO, corresponding to an increase in convection over eastern and southern Africa and reduced convection over Madagascar.

Further, Liu and Lu (2010) found an influence of the 11-year solar sunspot cycle on stratospheric and tropospheric circulation during winter (November to March) in the Northern Hemisphere, using re-analysis data for the meteorological fields. For example, for eastern QBO phases, the solar effects have an influence on the equatorial upper stratosphere and southern hemispheric stratosphere, where the enhanced solar ultraviolet radiation during high sunspot activity heats the stratospheric ozone layer, leading to an apparent increase in the temperature. Moreover, an analysis of monthly-scale variations in OLR led Hong et al. (2011) to conclude that the 11-year solar cycle and QBO significantly affect tropospheric convective activity around the near-Indonesian oceans.

In summary, MJO is the main forcing associated with precipitation. IOD is a dipole which is related to an increase in SST in one part of the Indian Ocean. This dipole varies in intensity from month to month and year to year. El Niño, even if it primarily affects the Pacific Ocean, seems to also affect the Indian Ocean by changing the zonal Walker circulation. Last of all, the eastern QBO phase, when associated with a maximum of the 11-year solar cycle, increases the temperature at the lower latitudes and also association with El Niño seems to change the zonal circulation between  $25$  and  $50^\circ \text{ E}$  in the lower latitudes.

One of the difficulties in identifying causality of the unusually large precipitation which was observed over the Indian Ocean in December 1991 is due to the complexity of these different forcings. As shown in this introduction, previous works have generally investigated one or two forcing processes at a time. In this paper, we try to look exhaustively at all possible forcing processes that may explain this anomalous precipitation period.

We try to address this question using meteorological observations from several islands in the Indian Ocean, from observations and satellite precipitation data (Global Precipitation Climatology Project (GPCP) monthly precipitation data set). Since the meteorological data are of high quality, this study should improve our knowledge of precipitation over the ocean, which shows considerable uncertainties in previous studies (e.g. Yin et al, 2004). Section 2 will present the description of the data used in this study. The associated anomalies of observed sunshine duration, temperature and precipitation across the different islands are described in Sect. 3.

The analysis of such anomalies will be done in Sect. 4 and concluding remarks are presented in Sect. 5.

## 2 Data description

### 2.1 Station location

Observations from seven islands in the Indian Ocean are used. Three islands are located in the tropics (Glorieuses, Mayotte, and Tromelin) with latitudes between  $11.30$  and  $15.53^\circ \text{ S}$ . One is a subtropical island (Réunion, at  $21.05^\circ \text{ S}$ ), and three are at higher latitudes (Nouvelle Amsterdam, the Crozet Islands and the Kerguelen Islands, situated between  $37$  and  $49^\circ \text{ S}$ ) (Fig. 1). Longitudes range from  $45.12^\circ \text{ E}$  (Mayotte) to  $69.20^\circ \text{ E}$  (Kerguelen Islands). To take into account the fact that sensors located near the centre of an island, or at higher altitude, are often cooler and dryer than the coastal regions (due to local dynamical conditions), only coastal stations located at sea level are considered so as to reduce the influence of the topography.

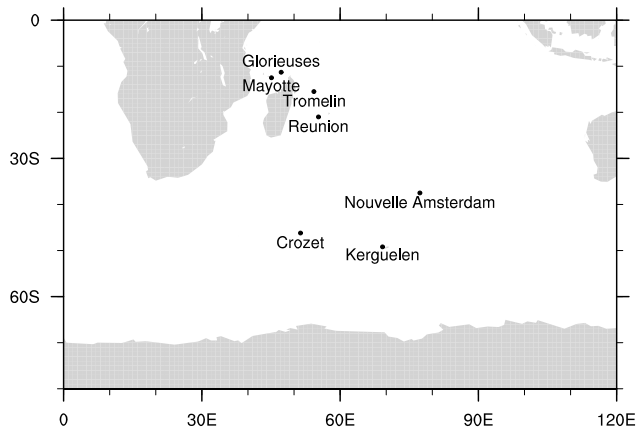


**Figure 1.** Map of the French islands in the Indian Ocean. The different coordinates are given from low to high latitudes: Glorieuses (47.2° E, 11.3° S), Mayotte (45.1° E, 12.5° S), Tromelin (54.3° E, 15.5° S), Réunion (55.3° E, 21.0° S), Nouvelle Amsterdam (77.3° E, 37.5° S), Crozet Islands (51.4° E, 46.2° S) and Kerguelen Islands (69.2° E, 49.2° S).

## 2.2 Characteristics of the data

### 2.2.1 In situ data

Data used in this study are the monthly (monthly mean of daily data) temperature, precipitation, and sunshine duration measurements acquired by the French national meteorological centre Météo France (Climatheque: <http://publitheque.meteo.fr/okapi/accueil/okapiWebPubli/index.jsp>) at each of the selected stations (Fig. 1). The rain is measured by rain gauges. The water falls into a receptacle and then into buckets which switch every 0.2 mm. Daily rain is the accumulation of rain that fell between 07:00 and 07:00 on the following day. Sunshine duration was primarily measured by the Campbell heliograph, a glass sphere that focuses sunlight on a strip of cardboard placed on a stand at the rear of the sphere. This produces a burning or discoloration of the board, the nature and structure of which are standardized. The board is changed every day. The length of the burn is measured with a ruler to estimate actual sunshine duration in hours and tenths. This device is simply named after its inventors (Campbell–Stokes sunshine recorder). After 1993, automated heliographs with a rotating electronic eye that records sunlight every minute started to be installed. In this case, sunshine exposure is considered to be present if the irradiance is greater than  $120 \text{ W m}^{-2}$ .

The temperature probe used to measure the temperature has an accuracy of  $0.15^\circ\text{C}$ . It is worth mentioning here that the weather parameters observed at some of these islands suffer from temporal inhomogeneities due to instrument modifications, as traditional sensors at many of these stations were replaced by automatic measuring instruments after December 1993. The automation was established two

and a half years after the Pinatubo eruption and therefore this change in the data should not affect our results.

Because sunshine duration data show some decreases associated with automation (changes of 30 % estimated by Météo France), the sunshine duration data cover slightly shorter periods than the precipitation and temperature data. This is the case for Nouvelle Amsterdam, Mayotte and Tromelin. Moreover, the lack of service staff since 2000 has led to a reduction in the number of available data after that year, in particular in the Glorieuses.

The different periods used in this study for the analysis are from 1 January 1964 to 31 December 2008 for Mayotte, Tromelin, Réunion, the Kerguelen Islands and Nouvelle Amsterdam. For the sunshine duration, the time series used for Nouvelle Amsterdam, Mayotte and Tromelin was only until December 2001. For the Crozet Islands, we use data from 1 January 1974 to 31 December 1993 and for the Glorieuses from 1 January 1966 to 31 December 1999 for all the parameters.

### 2.2.2 Satellite data

The monthly GPCP precipitation data set from 1979 to present combines observations (gauge measurements) and satellite precipitation data (<http://precip.gsfc.nasa.gov/>) into  $2.5^\circ \times 2.5^\circ$  global grids (Adler et al., 2003). The data sets from January 1979 until May 2014 are provided in several formats – daily, daily long-term series (between 1981 and 2010), monthly or long-term monthly (between 1981 and 2010). Here again, for consistency with the late 20th century climatologies studied here, long-term monthly values will be used (between 1979 and 1995). The spatial coverage is from  $88.75^\circ \text{ N}$  to  $88.75^\circ \text{ S}$  and from  $1.25$  to  $358.75^\circ \text{ E}$ .

### 2.2.3 MJO indices

MJO indices (MJO1–MJO10) associated with different longitudes ( $80, 100, 120, 140, 160^\circ \text{ E}$ ;  $120, 40, 10^\circ \text{ W}$ ; and  $20$  and  $70^\circ \text{ E}$ , respectively) are provided by the National Center for Environmental Prediction, Climate Prediction Center NCEP/CPC ([http://www.cpc.noaa.gov/products/precip/CWlink/daily\\_mjo\\_index/proj\\_norm\\_order.ascii](http://www.cpc.noaa.gov/products/precip/CWlink/daily_mjo_index/proj_norm_order.ascii)). Such indices are built through an extended empirical orthogonal function (EEOF) analysis from pentad (5-day) 200 hPa velocity potential anomalies equatorward of  $30^\circ \text{ N}$ . The MJO definition used here is as documented in Wheeler and Hendon (2004).

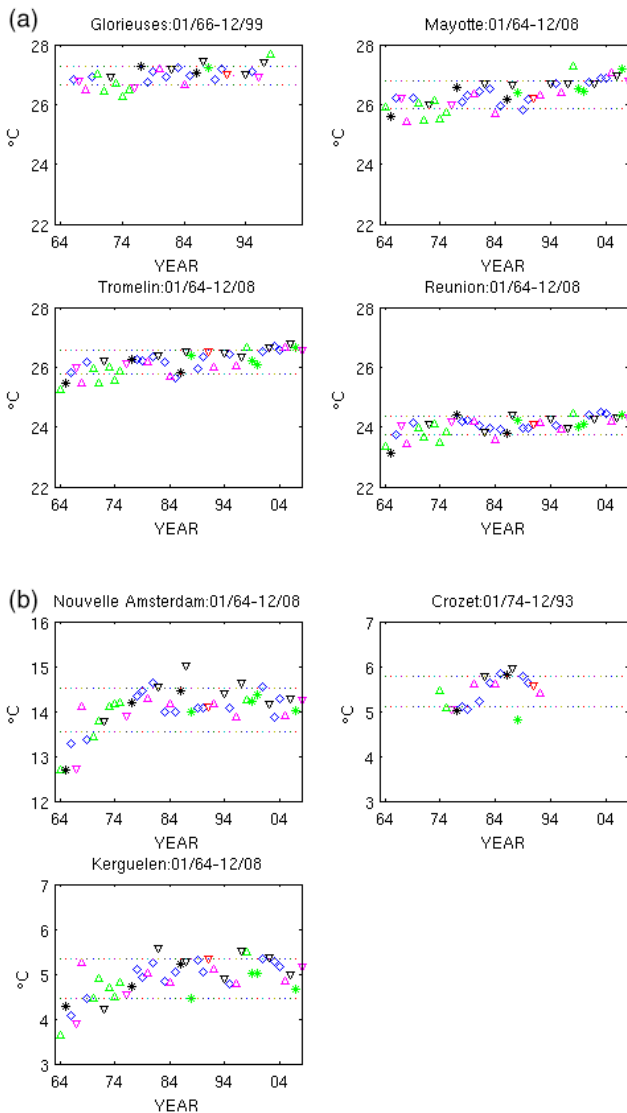


**Figure 2.** Time series of in situ measurements of mean yearly temperature at each island and the standard deviation (dotted). The red triangle is the 1991 (Pinatubo eruption) value. The others symbols are as follows: positive IOD – triangle down; negative IOD – triangle up; neither negative nor positive IOD – star. Green – La Niña; black – El Niño; magenta – neither La Niña nor El Niño. Years without any sign: diamond.

### 3 Evolution of the meteorological parameters on different islands in the southern Indian Ocean

#### 3.1 Temporal evolution of the meteorological parameters on different islands in the southern Indian Ocean

Annual mean temperature, precipitation and sunshine duration are shown in Figs. 2–4. The longest time series spans 45 years, from 1964 to 2008. As depicted in the temperature series, there has been a gradual temperature increase

since 1964 (e.g. around  $0.2^{\circ}\text{C decade}^{-1}$ ) (Fig. 2). In contrast, no systematic trend is observed in precipitation time series (Fig. 3). As expected, sunshine duration series exhibit a decreasing pattern as a function of latitude (Fig. 4). In the Glorieuses, Mayotte, and Tromelin islands, inter-annual variability of sunshine duration is moderate except in 1991 (red triangle), when average sunshine duration decreased by about  $1\text{ h day}^{-1}$ .

This negative peak is associated with high precipitation in the Glorieuses and Mayotte, where there more than  $150\text{ mm month}^{-1}$  occurs, instead of  $130\text{ mm month}^{-1}$ , which is the climatological mean (Fig. 3), but the corresponding temperatures do not show significant variations (Fig. 2). Note that there is a large peak in precipitation observed in the Glorieuses in 1978; this is associated with large precipitation in January, February and March brought by some tropical storms in those months. Further south, from Réunion to the Kerguelen Islands, sunshine duration, precipitation and temperature remained relatively stable during 1991 and the subsequent years.

#### 3.2 Seasonal evolution of the meteorological parameters on different islands in the southern Indian Ocean

The seasonal variations in precipitation, temperature and sunshine duration across different islands are depicted in Figs. 5–7. The Glorieuses, Mayotte and Tromelin have a typical inter-tropical climate with two well-defined seasons. From December to April (wet season), northerly winds are associated with heavy precipitation, as high as  $300\text{ mm month}^{-1}$  for Mayotte (Fig. 5). From May to September, southerly and easterly winds dominate the region, total precipitation is reduced, and the average temperature is around  $25^{\circ}\text{C}$  (Fig. 6). Réunion also has two distinct seasons: the warm ( $\approx 26^{\circ}\text{C}$ ), rainy ( $\approx 300\text{ mm month}^{-1}$ ) summer from December to April and the cool ( $\approx 22^{\circ}\text{C}$ ), dry ( $\approx 100\text{ mm month}^{-1}$ ) winter from late April to October. Réunion experiences easterly winds from April to October. However, Nouvelle Amsterdam is characterized by mild climatic conditions because of its location, north of the subtropical convergence zone (Lebouvier and Frenot, 2007). Strong westerly winds are frequent, especially in winter. The temperature is cooler on average (around  $12^{\circ}\text{C}$ ) from April to November, while it ranges between 15 and  $18^{\circ}\text{C}$  the rest of the year, when sunshine duration is lower (less than  $4\text{ h day}^{-1}$ ; Fig. 7). Heavy precipitation around  $100\text{ mm month}^{-1}$  occurs from March to September, and precipitation is less than  $80\text{ mm month}^{-1}$  during the dry season. Cloudiness is high all year round. The climate of the Crozet and Kerguelen islands is cold and windy. Mean annual air temperature is around  $5^{\circ}\text{C}$  with lower temperatures from May to October (less than  $6^{\circ}\text{C}$ ) and strong westerly winds are frequent. Sunshine duration is less than  $4\text{ h day}^{-1}$ , and temperature is around  $8^{\circ}\text{C}$  in summer. Precipitation is

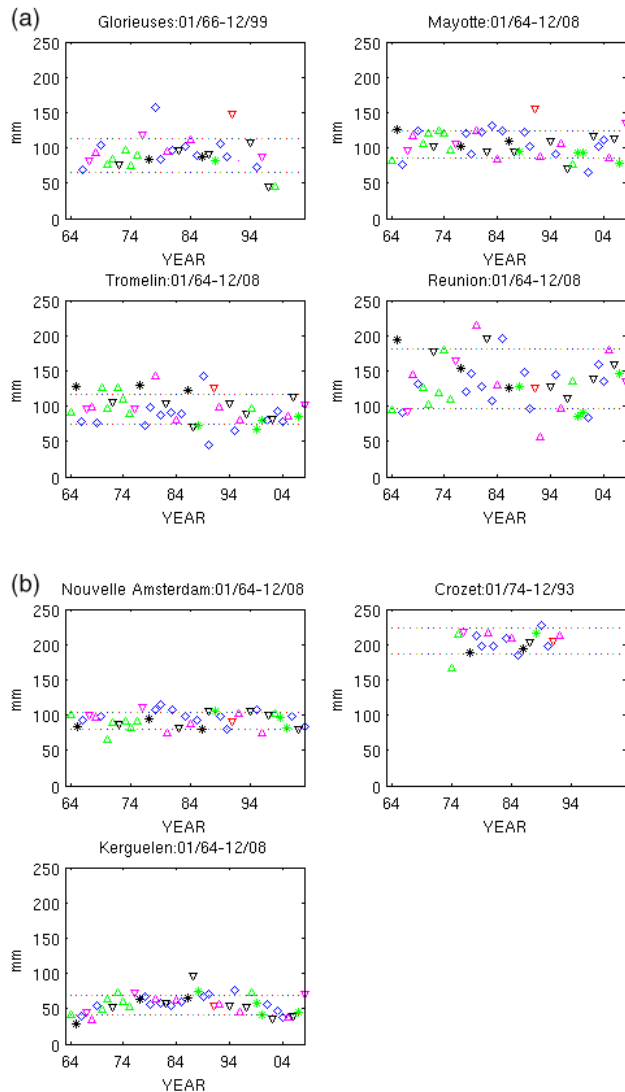


**Figure 3.** Same as Fig. 2 but for precipitation.

slightly higher from March to May. On average, the total annual amount of precipitation is around  $2400 \text{ mm yr}^{-1}$  for Nouvelle Amsterdam and  $760 \text{ mm yr}^{-1}$  at the Crozet and Kerguelen islands.

### 3.3 Anomalies of the different meteorological parameters after the Pinatubo eruption for the low-latitude islands

Precipitation, temperature and sunshine duration anomalies calculated for the period following the Pinatubo eruption (June 1991–May 1992) are also illustrated in Figs. 5–7. From June to December 1991, the duration of sunshine in the tropical islands was shorter than the corresponding climatological mean duration. In particular, very short sunshine duration occurred in December, especially in the Glorieuses and Mayotte (Fig. 7). It was only 5 h instead of the usual more than

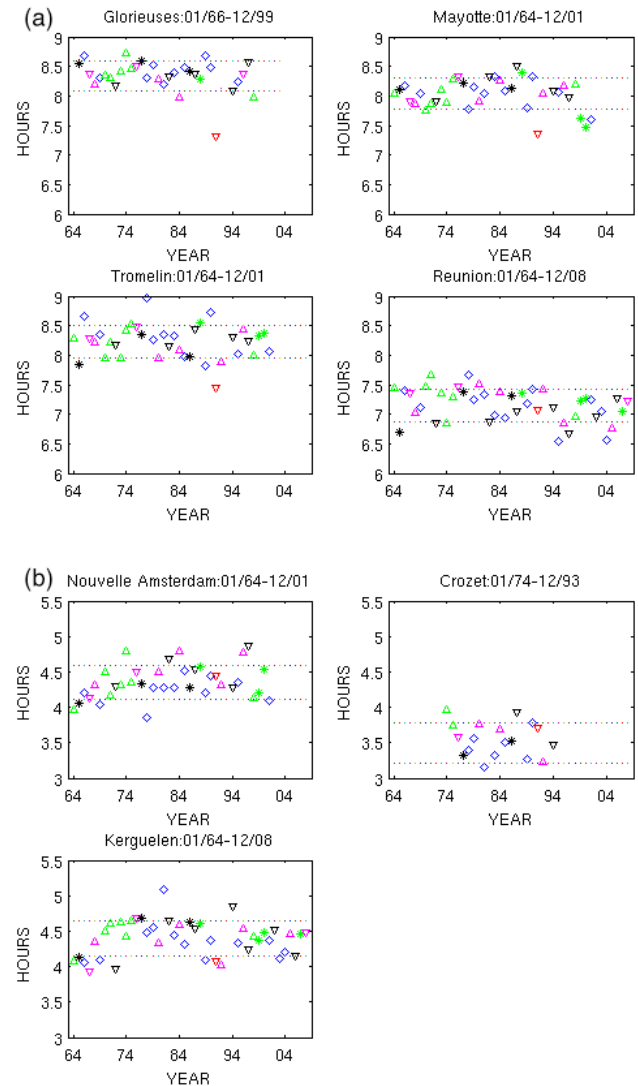


**Figure 4.** Same as Fig. 2 but for sunshine duration.

8.5 h in the Glorieuses and 6 h instead of the usual more than 7.5 h in Mayotte, which is significant at the 95 % level (i.e. outside the normal distribution, less than the mean minus  $2 \times$  standard deviation (SD)). In these islands, the short sunshine duration in December occurs together with a peak in precipitation (more than twice the climatological mean precipitation in the two islands, Fig. 5). Just after the Pinatubo eruption, shorter sunshine duration in Tromelin from June to October 1991 (around 6 h in July instead of more than 7 h in the climatology) is not correlated with higher precipitation. In the lower latitudes (Mayotte and Glorieuses), sunshine duration returns to a level close to the climatological mean by March 1992. For Tromelin, which is at higher latitude, sunshine duration is still perturbed in March 1992, when it is less than 6 h, compared to more than 7 h for the climatological mean. No significant deviation from climatology is observed in the temperature data (Fig. 6). This result differs from the temper-

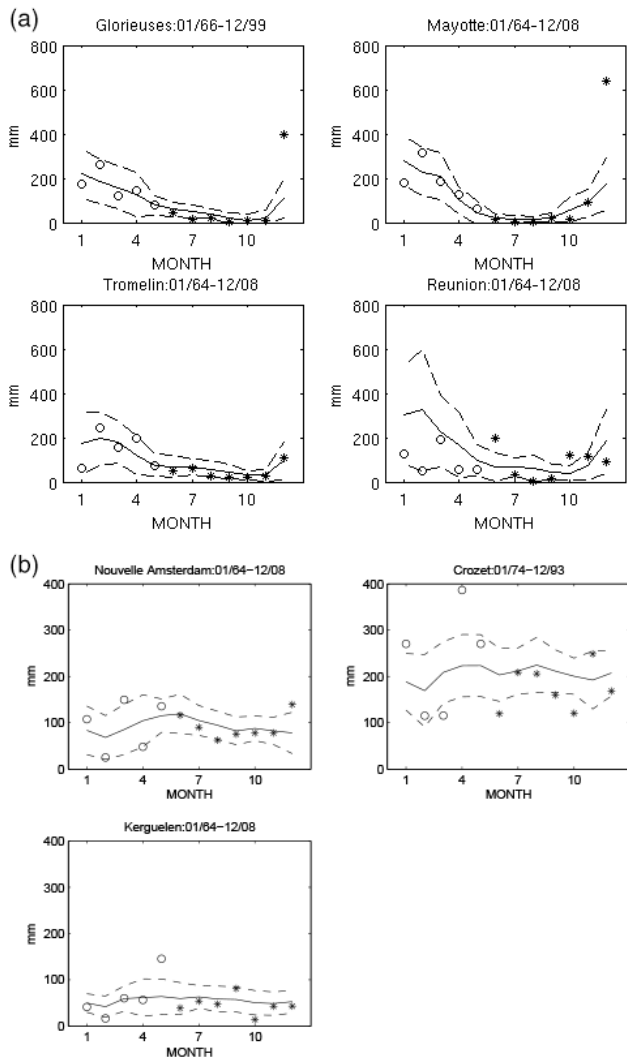


**Figure 5.** Comparison of climatological mean precipitation in the different islands and monthly mean precipitation following the Mount Pinatubo eruption from June to December 1991 (stars) and from January to May 1992 (circles) (a) for the lower-latitude islands (Glorieuses, Mayotte, Tromelin, Réunion) and (b) for the higher-latitude islands (Nouvelle Amsterdam, Crozet Islands, Kerguelen Islands). The solid and dashed lines show the mean values and the SD, respectively.

ature decrease observed after the eruption of Mount Pinatubo by Dutton and Christy (1992) at Mauna Loa Observatory on the island of Hawaii (19° N). In general, weather parameters (temperature, precipitation and sunshine duration) at higher latitudes (south of Réunion) were weakly affected and remained close to their corresponding climatological profiles during and after the eruption of Mount Pinatubo.

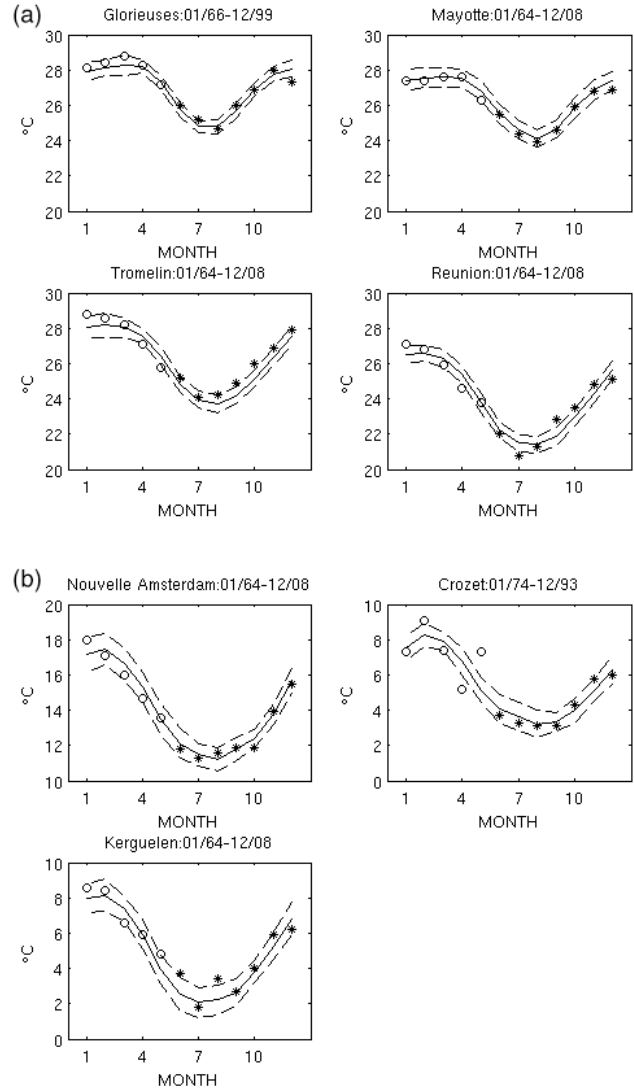


**Figure 6.** Same as Fig. 5 but for temperature.

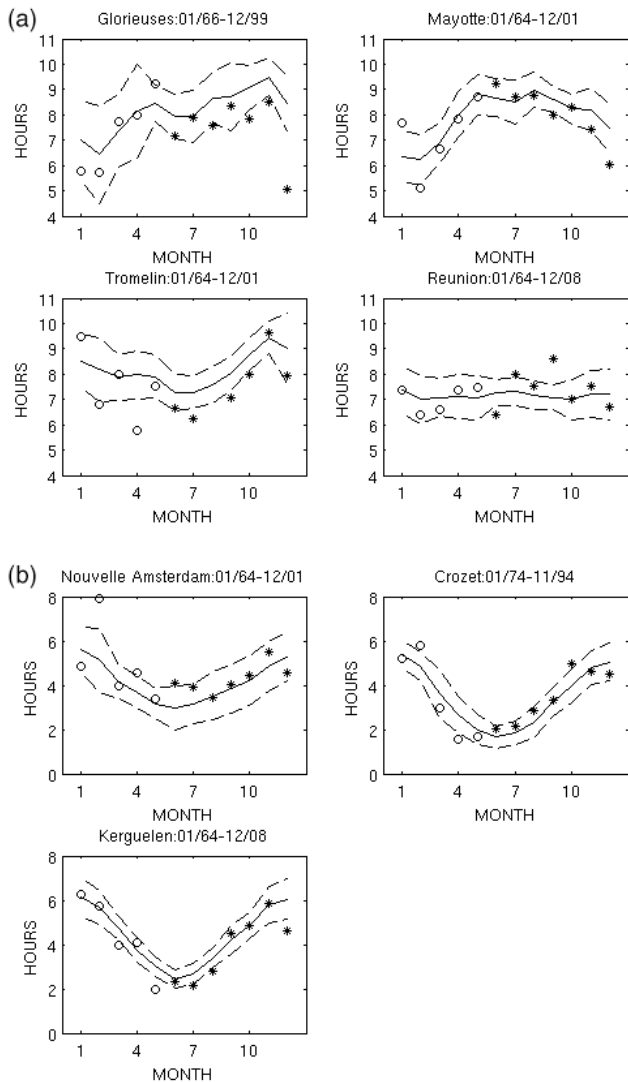
**4 Analysis of the precipitation and sunshine duration anomalies after the Pinatubo eruption for the low-latitude islands**

While El Chichón aerosols (28 March–4 April 1982) remained confined to 0 to 30° N latitude, the Pinatubo aerosols straddled the Equator (McCormic and Veiga, 1992; Stowe et al., 1992). This was partly due to the seasonal differences in their eruption periods, closer to winter for El Chichón and closer to summer for Pinatubo (Timmreck and Graf, 2006). In boreal winter, strong westerly winds dominate and transport aerosol air masses eastward and northward (during the El Chichón eruption). The cloud from a summer eruption is transported westward and more southward (Pinatubo eruption) due to the stratospheric Aleutian high, which drives the volcanic cloud towards the Equator. Schoeberl et al. (2008), analysing 13 years (1993 to 2005) of satellite data, observed



**Table 1.** Correlation coefficients ( $r$ ) between the meteorological data time series (**a** precipitation, **b** temperature) and the indices of the large scale oscillations (ENSO/SOI, IOD/DMI, QBO, SSN) and  $p$  value to test the hypothesis of no correlation.

<b>(a)</b>								
Forcings/precipitation	ENSO $r$	ENSO $p$	IOD $r$	IOD $p$	QBO $r$	QBO $p$	SSN $r$	SSN $p$
Glorieuses	-0.0571	0.2359	0.0293	0.5440	0.0890	0.0646	0.0495	0.3043
Mayotte	-0.0115	0.8121	0.0059	0.9020	0.1300	0.0068	0.0584	0.2256
<b>(b)</b>								
Forcings/temperature	ENSO $r$	ENSO $p$	IOD $r$	IOD $p$	QBO $r$	QBO $p$	SSN $r$	SSN $p$
Glorieuses	-0.1394	0.0037	0.0870	0.0710	0.1493	0.0019	0.0611	0.2054
Mayotte	-0.1800	0.0001	0.1277	0.0079	0.1384	0.0040	0.0049	0.9100

**Figure 7.** Same as Fig. 5 but for sunshine duration.

that, during the QBO's westerly phase, low-altitude (less than 22 km) aerosols and trace gases spread poleward, whereas during the QBO's easterly phase, lower-stratospheric trace

gases and aerosols remain near the Equator. Pinatubo erupted during the easterly phase of the QBO at 30 hPa, with a change to the westerly phase in August 1992 (Thomas et al., 2009). Therefore, the aerosol distribution may explain why lower sunshine duration was observed in the low-latitude Indian Ocean islands after the Pinatubo eruption. For instance, the Glorieuses, Mayotte and Tromelin experienced less sunshine duration than the average climatology after June. More particularly, sunshine duration in Tromelin was lower than the climatology from June to October and especially in July (about 6 h instead of 7.5 h in average). However, if this is the case, the data indicate a heterogeneous distribution of aerosols from the Pinatubo eruption over the 10–15° S latitude band, since the lower levels of sunshine duration which are observed are not the same on the Glorieuses, Mayotte and Tromelin. In higher-latitude islands (more than 20° S), sunshine duration did not decrease – i.e. islands further south than 20° S were not affected at all. Moreover, note that sunshine duration observed in Mayotte and the Glorieuses decreased strongly in December as precipitation increased. In the following sections, we will try to analyse whether these phenomena may be an effect of Pinatubo or whether different weather forcings could cause the increase in precipitation and decrease in sunshine duration in Mayotte and the Glorieuses.

#### 4.1 Spectral analysis

In order to determine the different (weather) forcings, we first apply spectral analysis to the temperature and precipitation records to identify typical periodicities in these data sets. (The noise level in sunshine duration records is very high, so they do not give useful spectral information.) We study the temperature spectra since several climate forcings affect the temperature first (see Introduction). Studying the temperature is relatively straightforward as it is the least noisy parameter.

To make it clear what periods are dominating, the most advanced multiple-taper method (MTM) has been used to estimate the power spectral density (PSD) of the variations in precipitation and temperature (Percival and Walden, 1993). This method uses linear or nonlinear combinations of modi-

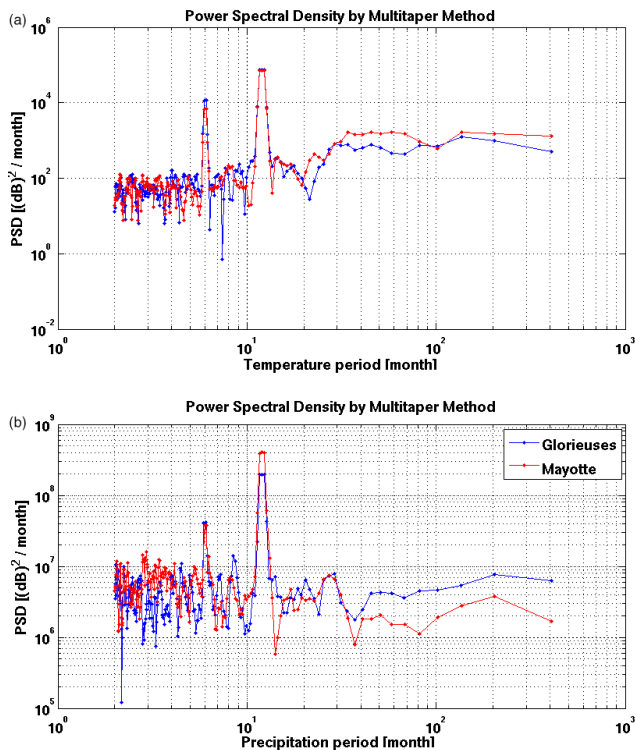


**Figure 8.** (a) Spectrum of temperature fluctuations ( $T$ ) obtained at the ground from January 1966 to December 1999. (b) Spectrum of precipitation fluctuations ( $P$ ) obtained at the ground from January 1966 to December 1999.

fied periodograms in order to minimize spectral leakage outside of the analysed spectral band. Figure 8a and b illustrate the PSD of the temperature and precipitation, respectively. Strong peaks at 12 and 6 months are clearly seen in the spectra, which are related to the annual and semi-annual variation in  $T$  and  $P$ . Also, another oscillation (although less intense) can be seen at about 30 months, which corresponds to the QBO.

The peak between 30 and 70 months (around 4 years) obtained from the temperature records and between 40 and 60 months for the precipitation should correspond to the ENSO and/or IOD oscillations. Larger peaks are obtained for the temperature between 100 and 200 months and for the precipitation around 200 months which correspond approximately to the solar cycle. Nevertheless, since the 11-year solar cycle and also MJO (1 to 2 months) are at the limits of the spectral range, they cannot be clearly observed in the PSD analysis.

#### 4.2 Correlation analysis: ENSO, IOD, QBO, SSN

In Table 1, we look at the simple correlation between precipitation and temperature and the ENSO (SOI), IOD (dipole mode index (DMI)), QBO and sunspot number (SSN) indices, using time series of monthly averages. (Note that the

timescale of changes in the MJO index is too short to make a similar correlation for the MJO.) Note that  $p$  tests the hypothesis of no correlation. Each  $p$  value is the probability of getting a correlation as large as the observed value by random chance when the true correlation is zero. If  $p$  is less than 0.05, the correlation  $r$  is significant at the 95 % level.

We find that the correlations with most indices and precipitation are not significant ( $p > 0.2$ ). Only the correlations with the QBO are significant ( $p = 0.06$  for the Glorieuses and 0.01 for Mayotte), but the correlation coefficients,  $r$ , are very small (0.09 and 0.13). It should be noted that Mayotte, with the slightly higher  $r$  value, is the most western island of our study.

This contrasts with the results of Jury et al. (1994). Using radiosonde profiles from 1960 to 1992, they showed correlations between QBO and tropospheric zonal wind anomalies at Mayotte, with QBO positively correlated with 200 hPa zonal winds over the western equatorial Indian Ocean. They also presented a schematic section for 5–20° S of the QBO as a mechanism for convective modulation over eastern and southern Africa and the SW Indian Ocean. Strong correlations were found for summer over Madagascar, such that, when the QBO was from west, there was a reduction in clouds. The QBO was associated with a convective dipole with ascending/descending nodes at 25° E/50° E in the subtropical latitude band, which would be expected to give a negative correlation between QBO and rainfall.

Although, in the present study, the correlation between precipitation and SOI index is not significant at the 95 % level, the sign of  $r$  (Table 1a) does suggest that precipitation, if anything, is anti-correlated with SOI index, which is in agreement with past results. This is in agreement with Webster et al. (1999), who found that rainfall in the western Indian Ocean is larger during El Niño events.

Considering correlations with temperature (Table 1b), we find that the correlation with SSN is very weak and the result non-significant ( $p > 0.2$ ); however, with QBO, IOD and ENSO, the correlations are significant ( $p < 0.07$ ) and the correlation coefficients are also larger than 0.08 in absolute value. Our results are in contradiction with Jury et al. (1994), who found that the SOI index and QBO were not correlated with SST but instead only 200 hPa zonal winds.

The correlation with IOD and the temperature for the Glorieuses is the weakest. In the composites of the SST anomalies for July–November of 1994, 1997 and 2006 (positive IOD) realized by Abram et al. (2008), the Glorieuses were weakly affected by the IOD, which can explain this small contribution to the temperature. Here the SOI index is also anti-correlated with temperature, which is in agreement with most results published in the literature. As discussed by Kuleshov et al. (2009), ENSO induces anomalous circulation in the Indian region. ENSO affects the intensity of the easterly winds as well as the SST and the relative humidity in the middle troposphere and thus changes Walker circulation. Positive (negative) anomalies of SST can be observed

**Table 2.** Classification of years when El Niño or La Niña (presence during the second part of the year) and/or a positive or negative Indian Ocean Dipole occurred (when DMI index exceeds  $1\sigma$  above or below zero during the last part of the year for at least 2 or 3 months).

	Negative IOD	No event	Positive IOD
El Niño		65, 77, 86, 93	72, 82, 87, 91, 94, 97, 02, 06
No event	68, 80, 84, 85, 92, 96, 05	66, 69, 78, 79, 81, 83, 89, 90, 95, 01, 03, 04	67, 76, 08
La Niña	64, 70, 71, 73, 74, 75, 98	88, 99, 00, 07	

in the equatorial western part of the Indian Ocean during El Niño (La Niña). However, simple correlation analysis with single forcing indices may not represent all aspects of the possible influence of these forcings (for example, it does not tell us how they might affect variability in rainfall). Therefore, to complete this analysis, the link between temperature, precipitation and sunshine duration on a year-by-year basis, as a function of the different states of the different forcings (high/low) is next examined for Mayotte and the Glorieuses.

### 4.3 El Niño/IOD forcing

#### 4.3.1 Characteristics of the years as a function of El Niño and IOD

The preliminary analysis above indicates significant effects of ENSO and IOD on the different weather data sets. In the present analysis, a given year is identified as La Niña/El Niño, or IOD positive/negative, when the threshold value of the appropriate index (SOI or DMI) exceeds  $1\sigma$  above or below zero during the last part of the year for at least 2 or 3 months. Results from our analysis are presented in Table 2. There are noticeable differences between our results (e.g. the strong positive IOD phase during 1987) compared to those reported in Meyers et al. (2007). The selection of Meyers et al. (2007) is rather different since the time series in their analysis are filtered with a 5-month running mean and the IOD years are identified as those when the index was outside  $\pm\sigma$  for 2 months between June and December, with the years of La Niña/El Niño identified as those when the index was outside  $\pm\sigma$  for 2 months between June and February. In Table 2, it is also clear that positive IOD was often associated with El Niño (as reported in Saji and Yamagatta, 2003), while La Niña is more related to a negative IOD.

#### 4.3.2 Influence of El Niño on the meteorological parameters in Mayotte and the Glorieuses

Table 3a and b show the mean and SD of precipitation in December associated with IOD positive, IOD negative, El Niño and La Niña for the Glorieuses and Mayotte, respectively. The analyses were made using data from before 2000 in the Glorieuses and Mayotte, since the data are not good enough later. From the table it can be seen that there was enhanced precipitation in December during the periods of positive IOD and El Niño (precipitation around  $190 \pm 135$  mm

in the Glorieuses and  $279 \pm 227$  mm in Mayotte) compared to the mean precipitation in December for all of the studied period ( $109 \pm 85$  in the Glorieuses and  $174 \pm 118$  mm in Mayotte).

Nevertheless, considering the SD, it may be noted that the mean value obtained during the different forcings is not really representative, since there is a lot of dispersion in the data (large SD). Therefore, during such forcing (IOD+, El Niño), there can be a lot of precipitation as well as much less than average. This is likely because the ascending branch of Walker cell in the Indian Ocean is very dependent on the dynamic circulation since it is moving a lot.

During El Niño, the ascending Walker branch is closer to or further from South America depending on the year. As a function of the intensity of El Niño, the Walker branch is smaller or larger and also depends strongly on the MJO circulation (Takayabu et al., 1999), which could explain the high variability of the rain in Mayotte and the Glorieuses during El Niño.

Conversely, there was less precipitation during negative IOD and La Niña (pure or not) phases ( $111 \pm 66$  mm in the Glorieuses and  $132 \pm 86$  mm for Mayotte), but here, again, such difference in the mean precipitation observed during all the months is not large considering the SD. Nevertheless, there is a lower SD in this case than during positive IOD and El Niño, even if the number of the years analysed in each state is nearly the same (eight for IOD+ El Niño and seven for IOD– La Niña). In fact, during La Niña, the ascending branch of the Walker circulation is closer to Indonesia, so the other ascending branch of the Walker cell is far from the longitudes of Mayotte and the Glorieuses, particularly during December in many years, and thus there is less precipitation.

While IOD or El Niño should affect the temperature (El Niño is defined as a decrease in the pressure in the eastern part of the Pacific Ocean due to an increase in surface temperature and IOD is defined as an anomaly of temperature in the western part of the Indian Ocean), the analysis of the observations does not show any significant differences in temperature in the Glorieuses and Mayotte (Table 3c–d) during December according to El Niño and IOD phases. All of the temperatures are close to  $28.1^\circ\text{C}$  in the Glorieuses and  $27.4^\circ\text{C}$  in Mayotte. However, they are slightly higher during El Niño and IOD+ for the Glorieuses ( $+0.1^\circ\text{C}$ ) and lower during La Niña and IOD– ( $-0.6$  and  $-0.5^\circ\text{C}$  for the Glorieuses and Mayotte, respectively). This difference is even

**Table 3.** Mean and SD of precipitation (mm month<sup>-1</sup>) in December for (a) the Glorieuses and (b) Mayotte during the different phases of ENSO and IOD, and mean and SD of temperature (°C) for (c) the Glorieuses and (d) Mayotte during the different phases of ENSO and IOD.

(a) Glorieuses (precipitation)			
Mean: 109 ± 85	IOD+	IOD–	Unqualified
El Niño	190 (±135)		81 (±46)
La Niña		111 (±66)	44 (±20)
Unqualified	79 (± 29)	55 (±46)	106 (±82)
(b) Mayotte (precipitation)			
Mean: 174 ± 118	IOD+	IOD–	Unqualified
El Niño	279 (±227)		161 (±47)
La Niña		132 (±86)	99 (±17)
Unqualified	174 (±154)	102 (±47)	193 (±104)
(c) Glorieuses (temperatures)			
Mean: 28.1 (±0.5)	IOD+	IOD–	Unqualified
El Niño	28.2 (±0.7)		28.2 (±0.4)
La Niña		27.5 (±0.5)	28.4 (±0.0)
Unqualified	28.0 (±0.1)	28.0 (±0.3)	28.2 (±0.3)
(d) Mayotte (temperatures)			
Mean: 27.4 (±0.5)	IOD+	IOD–	Unqualified
El Niño	27.4 (±0.5)		27.2 (±0.4)
La Niña		26.9 (±0.5)	27.6 (±0.4)
Unqualified	26.9 (±0.3)	27.2 (±0.4)	27.4 (±0.2)

**Table 4.** Classification of years when SSN max or SSN min and/or western or eastern QBO occurred.

	SSN max	SSN min	Others
Western QBO phase	69, 78, 80, 90, 99, 02	64, 73, 75, 85, 87, 95, 97, 06, 08	66, 71, 82, 92, 04
Eastern QBO phase	67, 68, 70, 79, 81, 89, 91, 00	65, 74, 76, 86, 96, 05, 07	72, 98, 03
Others	01	77, 94	83, 84, 88, 93

higher in the Glorieuses, which are further east in the Indian Ocean and thus closer to the centre of action of IOD; considering the SD (which is higher than the differences), this difference is not significant since it is less than the standard deviation, which is very large. This is possibly due to the fact that such islands are in the middle of the ocean or that El Niño and IOD+ act more on the precipitation on the different islands.

This means that, if such forcings act on the precipitation on the two islands, it is more by an indirect mechanism, for example through the large-scale circulation, not by a local effect on temperature.

Mayotte and the Glorieuses recorded high precipitation (400 and 600 mm, respectively; see Fig. 5) during December 1991. In 1991, the SOI was negative in December and even more so in January and February. As we see in Table 3, negative SOI (El Niño) is on average associated with higher

precipitation. However, from looking at the rain each year in Tromelin, Mayotte and the Glorieuses (Fig. 3), it can be seen that the years of El Niño were not all associated with extreme rainfall in December. For example, although there was El Niño during 1997, the month of December was extremely dry.

Often, at the end of the year the DMI changes sign, which should not lead to a strong influence of the dipole on precipitation behaviour in December. (Although the IOD often decreases in December/January, which means that the IOD effect is weaker, for completeness we have also considered the influence of the IOD in addition to the impact of ENSO on precipitation in December.) The DMI is often smaller in December than during the rest of the year, although the precipitation in all cases is more during the years of IOD+ phase than the mean precipitation observed over the whole year, both in the Glorieuses and Mayotte. Even if it is the end of

**Table 5.** Mean and SD of precipitation ( $\text{mm month}^{-1}$ ) in December for (a) the Glorieuses and (b) Mayotte during the different phases of QBO and SSN, and mean and SD of temperature ( $^{\circ}\text{C}$ ) for (c) the Glorieuses and (d) Mayotte during the different phases of QBO and SSN.

(a) Glorieuses (precipitation)			
Mean: $109 \pm 85$	SSN max	SSN min	Unqualified
Eastern QBO phase	141 ( $\pm 11$ )	90 ( $\pm 51$ )	95 ( $\pm 124$ )
Western QBO phase	59 ( $\pm 33$ )	96 ( $\pm 71$ )	105 ( $\pm 93$ )
Unqualified	15	126 ( $\pm 155$ )	114 ( $\pm 125$ )
(b) Mayotte (precipitation)			
Mean: $174 \pm 118$	SSN max	SSN min	Unqualified
Eastern QBO phase	252 ( $\pm 181$ )	114 ( $\pm 75$ )	110 ( $\pm 34$ )
Western QBO phase	132 ( $\pm 61$ )	120 ( $\pm 71$ )	248 ( $\pm 167$ )
Unqualified	86	161 ( $\pm 91$ )	167 ( $\pm 135$ )
(c) Glorieuses (temperatures)			
Mean: $28.1 \pm 0.5$	SSN max	SSN min	Unqualified
Eastern QBO phase	27.9 ( $\pm 0.5$ )	27.9 ( $\pm 0.4$ )	28.4 ( $\pm 0.2$ )
Western QBO phase	28.2 ( $\pm 0.3$ )	28.0 ( $\pm 0.8$ )	27.9 ( $\pm 0.2$ )
Unqualified	28.5	28.0 ( $\pm 0.1$ )	28.2 ( $\pm 0.2$ )
(d) Mayotte (temperatures)			
Mean: $27.4 \pm 0.5$	SSN max	SSN min	Unqualified
Eastern QBO phase	27.1 ( $\pm 0.6$ )	27.2 ( $\pm 0.4$ )	27.7 ( $\pm 0.3$ )
Western QBO phase	27.3 ( $\pm 0.2$ )	27.3 ( $\pm 0.6$ )	27.2 ( $\pm 0.3$ )
Unqualified	28.3	27.3 ( $\pm 0.3$ )	27.3 ( $\pm 0.2$ )

the IOD+ phase, the global circulation brings precipitation to these two islands. It is as if the global circulation reacts more slowly than the change of the surface circulation.

The very high values of precipitation in 1991 were higher than any previous values (since 1964) and should be attributed to some other phenomena than El Niño/IOD alone.

#### 4.4 QBO/SSN forcing

Table 4 shows the division of observation years according to the state of the sunspot number (SSN) and QBO. Earth's global climate can be affected by the changes in solar energy output between solar minima (low SSN) and solar maxima (high SSN). Table 5a and b show how the precipitation depends on QBO phase and SSN. During maximum solar activity and the eastern QBO phase, there is more precipitation than during the western QBO phase (Table 4), which is in agreement with the work reported in Liu and Lu (2010). Furthermore, the total precipitation was stronger during SSN maximum and the eastern QBO phase (i.e.  $141 \pm 111$  and  $252 \pm 181$  mm at the Glorieuses and Mayotte, respectively) than for all the other conditions in the two islands. Again, considering the high SD during the eastern QBO/high SSN, the mean precipitation is not really representative, and during such forcings there can be a lot of rain as well as very

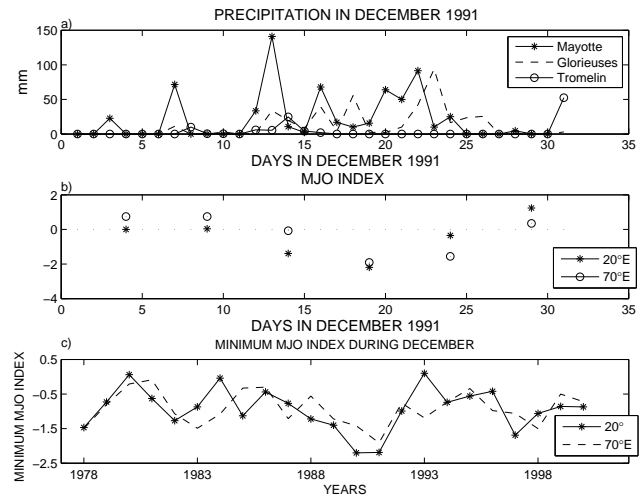


**Figure 9.** Time series of (a) precipitation in December 1991 for the Glorieuses, Mayotte and Tromelin and (b) the MJO index at 20 and 70° E. Pentad MJO indices for 1991 are derived from extended empirical orthogonal function (EEOF) analysis applied to pentad 200 hPa velocity potential (CHI200) anomalies equatorward of 30° N during ENSO-neutral and weak ENSO winters (November–April). (c) Minimum of MJO index observed each year during December.

little. Nevertheless, the two forcings SSN and QBO have not, in other years, led to such large amounts of precipitation as obtained in December 1991. Moreover, the temperatures recorded during the different forcing conditions (Table 5c–d) are quite similar and, if anything, are lower during SSN max and QBO easterly than during others forcings (27.9 and 27.1  $^{\circ}\text{C}$  in the Glorieuses and Mayotte, respectively, although the mean temperatures are 28.1 and 27.4  $^{\circ}\text{C}$ ). As QBO or SSN has more influence in the upper troposphere, it more affects the motion at such levels rather than the surface temperature. This means that, if such forcings act on the precipitation at the two islands, it is by an indirect mechanism through the large-scale circulation. These findings suggest that temperature changes could occur higher up, modifying dynamics, as already observed in many studies.

In conclusion, as summarized in Tables 1, 3 and 5, we could not find any clear evidence of an effect of any of the forcings (ENSO, IOD, QBO or SSN), which could explain the anomalous precipitation observed in the Glorieuses and Mayotte during December 1991. However, over the period 1964–2008, only 1991 exhibited an anomalous El Niño and a positive IOD, eastern QBO phase and SSN max. Both of these pairs of forcings are associated with higher mean precipitation and higher variability in the precipitation. The observed precipitation in December 1991 lies between 2 and 3 SDs above the mean for each pair – if the effects are additive, they could in principle be together responsible for the observed anomaly with a few percent probability.

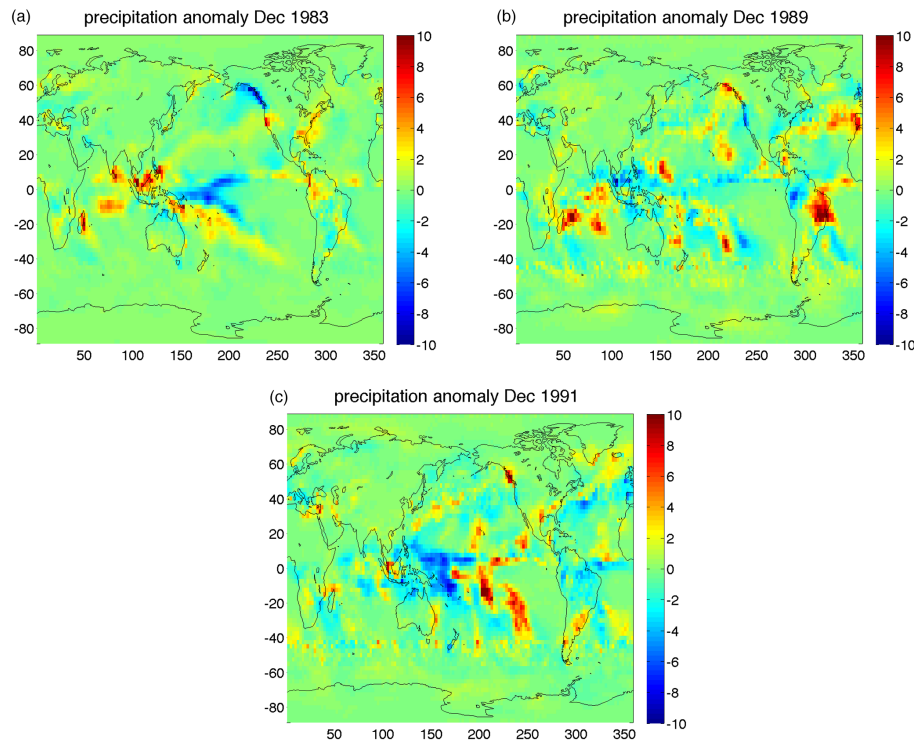


**Figure 10.** Anomalies of precipitations in December 1983 (a), 1989 (b) and 1991 (c) (December 1983, 1989 and 1991 minus December 1979–1995) from the GPCP data set.

#### 4.5 MJO forcing

To investigate how MJO may affect the precipitation, the daily precipitation observed in December in the Glorieuses, Mayotte and Tromelin is compared with the MJO index (Wheeler and Hendon, 2004) at 20° and 70° E (see Fig. 9a, b).

The choice to take Tromelin as well, although there are no anomalies of precipitation there in December, is to show that precipitation in Tromelin is not correlated with MJO, although there is a very good correlation between the precipitation observed in Mayotte and the Glorieuses and the MJO. Moreover, since the Glorieuses are further east than Mayotte, it is closer to the signal observed at 70° E, and the rain appears later (it begins and finishes later) on the Glorieuses since the MJO propagates eastward. The fact that, in higher latitudes, Tromelin seems to not be influenced by the MJO can also explain why the sunshine duration is not affected on this island in December.

Therefore, the MJO index is correlated with precipitation in December 1991 at Mayotte and the Glorieuses. Examination of the MJO index at 20° and 70° E, for the months of December for every year from 1978 to 2000 (Fig. 9c), shows that December is often affected by periods of negative MJO index with varying amplitudes and duration. Nevertheless, in 1991, the index observed at 20° and 70° E was more extreme than in most other years. On 19 December, the MJO reached  $-2.19$  and  $-1.9$ , respectively, and was associated

with 638.3 mm of rain in Mayotte and 396.1 mm of rain in the Glorieuses. However, during December 1990 (Fig. 9c), the MJO index at 20° E was as low,  $-2.2$ , but Mayotte had only 108.4 mm of rain (and at 70° E the MJO index was not as low,  $-1.42$ , and the Glorieuses had only 97.1 mm of rain). Thus the extreme December minimum of the MJO index in 1991 was exceptional, and unique in that it affected both longitudes (20° and 70° E).

Figure 10 shows the latitude–longitude distribution of anomalies of precipitation for the month of December 1991 as well as 1983 and 1989 from the GPCP satellite. Even if the higher precipitation observed in Mayotte and the Glorieuses is not entirely local (there is a small zone of precipitation from 40 to 60° E and around 10° S), the anomalous precipitation is not as widespread as might be expected if it is associated with large-scale motions created by the Pinatubo influence (e.g. change in radiative forcing under the volcanic cloud which should perturb the thermodynamic balance of the climatic system) and looks rather to be associated with MJO forcing. Moreover, in 1983 and 1989, which are also affected in December by negative MJO, similar localized anomalies of precipitation can be observed (for example localized in the middle of the Indian Ocean in 1983) which are larger and more intense than 1991. This shows that anomalies would have occurred even if there had not been a Pinatubo eruption.

According to Trenberth and Day (2007), there was a decrease in precipitation over land and a record decrease in runoff and river discharge into the ocean from October 1991 to September 1992 due to the attenuation of solar radiation by the volcanic cloud. This decreased the atmospheric heating, which altered the latent heat release (Trenberth and Stepaniak, 2004). Such an attenuation of solar radiation is immediately more readily observable over the continent than over the ocean, so there should be more rain occurring over the ocean than over the continents. This is observed in Fig. 10 (1991) for the east of South America and Australia, but in Africa there is more precipitation that year around 20° S on the continent.

According to Jury et al. (1994), the western phase of the QBO strengthens the convective dipole between eastern and southern Africa and the SW Indian Ocean to bring stronger subsidence and less precipitation in the Glorieuses and Mayotte. The eastern phase of the QBO which prevailed in 1991 might then be expected to do the opposite, i.e. weakening subsidence, allowing convection and increasing precipitation, and this should be increased by the action of the MJO effect.

## 5 Conclusions

This paper has examined possible effects of the Pinatubo eruption on the climatic variables total precipitation, temperature and sunshine duration for Indian Ocean islands against the background of other weather forcings (ENSO, IOD, QBO, SSN, MJO). The potential impacts of this eruption can be summarized as follows:

1. Sunshine duration on the tropical islands Tromelin, the Glorieuses and Mayotte decreased from June 1991 until March 1992. This might be the result of the Pinatubo eruption, which injected aerosols into the atmosphere, increasing optical depth over the islands just after the eruption. If the changes in sunshine duration are due to the direct effect of the volcanic aerosol, then the data show that the distribution of aerosol from the volcanic eruption was not homogeneous over the 10–15° S latitude band, since the effects on the sunshine duration are different on the different islands (since Mayotte was not really affected from July to August).
2. The temperatures recorded in the different islands (even in the tropics) after the Pinatubo eruption were close to the climatological mean values, i.e. not affected by the Pinatubo eruption, in contrast to the sunshine duration parameter, even though various other studies (e.g. by Robock and Mao, 1995) have associated volcanic eruptions with colder temperature. Ramanathan (1988) also demonstrated a tropospheric radiative impact (a decadal radiative cooling) due to the El Chichón eruption in April 1982. The small decline in temperature could be

attributed to the spatial extent and location of the islands considered in the present study; that is, they are small and located in the middle of the ocean in the Southern Hemisphere, which was less directly affected by SO<sub>2</sub> emission from the volcano, and there were fewer temperature variations, due to the strong calorific capacity of the water.

3. Higher precipitation and weak sunshine duration observed during December 1991 at Mayotte and the Glorieuses seem to be more correlated to the MJO than to other forcings (influence of Pinatubo and meteorological forcings), although other meteorological forcings (i.e. El Niño, positive IOD, easterly QBO and SSN max) may have contributed to the increase in precipitation (high SDs are associated with the different forcings).

The MJO index was very low during December in both 1990 and 1991, but strong precipitation was observed only in 1991. However, the other forcings also may not have direct but instead indirect effects, for example modulating the convective dipole between southern Africa and Madagascar and adding to the MJO, in a way which could bring more precipitation to the Glorieuses and Mayotte in 1991 than in 1990.

Since MJO interacts with the ocean, it is strongly influenced by and itself influences ENSO, so it is really not possible to separate the influence of MJO from El Niño in this case of precipitation.

Islands at higher southern latitudes than 15.5° S were not affected by MJO in terms of sunshine duration, precipitation or temperature.

A comparison with a climatic model which simulates correctly MJO and others forcings would be necessary to complete our analysis. Such an analysis is needed to elucidate the importance of the different climate forcings and their interconnections. Better understanding of the different mechanisms should allow for better climate simulations in future.

*Acknowledgements.* This research is funded by the ANR programme “interface” and supported by TAAF (French Austral and Antarctic Territory) and FAZSOI (French South Indian Ocean Armed Forces). We acknowledge Météo France for providing in situ data and more particularly all the climatology team for their valuable help. GPCP precipitation data are provided by NOAA/OAR/ESRL PSD, Boulder, Colorado, USA, from their website at <http://www.esrl.noaa.gov/psd/>. We also want to thank the Physical Sciences Division, ESRL (NOAA), for the production of the data used in this research project. Lastly, we extend our thanks to P. Bechtold from ECMWF for his frequent help, as well as A. Robock, K. E. Trenberth, P. Keckhut, J. P. Cammas and S. Bielli for many suggestions.

The topical editor V. Kotroni thanks two anonymous referees for help in evaluating this paper.

## References

- Abram, N. J., Gagan, M. K., Hantoro, W. S., and Mudelsee, M.: Recent intensification of tropical climate variability in the Indian Ocean, *Nat. Geosci.*, 1, 849–853, doi:10.1038/ngeo357, 2008.
- Adler, R. F., Huffman, G. J., Chang, A., Ferraro, R., Xie, P., Janowiak, J., Rudolf, B., Schneider, U., Curtis, S., Bolvin, D., Gruber, A., Susskind, J., and Arkin, P.: The Version 2 Global Precipitation Climatology Project (GPCP) Monthly Precipitation Analysis (1979–Present), *J. Hydrometeorol.*, 4, 1147–1167, 2003.
- Ashok, K., Guan, Z., and Yamagata, T.: A look at the relationship between the ENSO and the Indian Ocean Dipole, *J. Meteorol. Soc. JPN*, 81, 41–56, 2003.
- Ashok, K., Guan, Z., Saji, N. H., and Yamagata, T.: Individual and combined influences of the ENSO and Indian Ocean Dipole on the Indian summer monsoon, *J. Climate*, 17, 3141–3155, 2004.
- Baldwin, M. P., Gray, L. J., Dunkerton, T. J., Hamilton, K., Haynes, P. H., Randel, W. J., Holton, J. R., Alexander, M. J., Hirota, I., Horinouchi, T., Jones, D. B. A., Kinnersley, J. S., Marquardt, C., Sato, K., and Takahashi, M.: The Quasi-Biennial Oscillation, *Rev. Geophys.*, 39, 179–229, 2001.
- Behera, S. K. and Yamagata, T.: Influence of the Indian Ocean Dipole on the Southern Oscillation, *J. Meteorol. Soc. JPN*, 81, 169–177, 2003.
- Behera, S. K., Krishnan, R., and Yamagata, T.: Unusual ocean-atmosphere conditions in the tropical Indian Ocean during 1994, *Geophys. Res. Lett.*, 26, 3001–3004, 1999.
- Behera, S. K., Rao, S. A., Saji, H. N., and Yamagata, T.: Comments on “A cautionary note on the interpretation of EOFs.”, *J. Climate*, 16, 1087–1093, 2003.
- Bluth, G. J. S., Doiron, S. D., Schetzler, S. C., Krueger, A. J., and Walter, L. S.: “Global Tracking of the SO<sub>2</sub> Clouds from the June 1991 Mount Pinatubo Eruptions.”, *Geophys. Res. Lett.*, 19, 151–154, 1992.
- Broccoli, A. J., Dixon, K. W., Delworth, T. L., Knutson, T. R., Stouffer, R. J., and Zeng, F.: Twentieth-century temperature and precipitation trends in ensemble climate simulations including natural and anthropogenic forcing, *J. Geophys. Res.*, 108, 4798, doi:10.1029/2003JD003812, 2003.
- Chang, P., Yamagata, T., Schopf, P., Behera, S. K., Carton, J., Kessler, W. S., Meyers, G., Qu, T., Schott, F., Sheptye, S., and Xie, S.-P.: Climate Fluctuations of Tropical Coupled Systems – The Role of Ocean Dynamics, *J. Climate*, 19, 5122–5174, 2005.
- Church, J. A., White, N. J., and Arblaster, J. M.: Significant Decadal-Scale Impact of Volcanic Eruptions on Sea Level and Ocean Heat Content, *Nature*, 438, 74–77, 2005.
- Curtis, S. and Adler, R. F.: Evolution of El Niño-precipitation relationships from satellites and gauges, *J. Geophys. Res.*, 108, 4153, doi:10.1029/2002JD002690, 2003.
- Dutton, E. G. and Christy, J. R.: Solar Radiative Forcing at Selected Locations and Evidence for Global Lower Tropospheric Cooling Following the Eruption of El Chichón and Pinatubo, *Geophys. Res. Lett.*, 19, 2313–2316, 1992.
- Elleman, R.: Predicting the Madden and Julian Oscillation Using a Statistical Model, unpublished, 1997.
- Fueglistaler, S., Dessler, A. E., Dunkerton, T. J., Folkins, I., Fu, Q., and Mote, P. W.: Tropical tropopause layer, *Rev. Geophys.*, 47, RG1004, doi:10.1029/2008RG000267, 2009.
- Hofmann, D. J.: Perturbations to the Global Atmosphere Associated with the El Chichón Volcanic Eruption of 1982, *Rev. Geophys.*, 25, 743–759, 1987.
- Hong, P. K., Miyahara, H., Yokoyama, Y., Takahashi, Y., and Sato, M.: Implications for the low latitude cloud formations from solar activity and the Quasi-Biennial Oscillation, *J. Atmos. Sol.-Terr. Phys.*, 73, 587–591, doi:10.1016/j.jastp.2010.11.026, 2011.
- Jones, C., Waliser, D. E., and Gautier, C.: The influence of the Madden-Julian Oscillation on ocean surface heat fluxes and sea-surface temperatures, *J. Climate*, 11, 1057–1072, 1998.
- Jones, P. D., Moberg, A., Osborn, T. J., and Briffa, K. R.: Surface climate responses to explosive volcanic eruptions seen in long European temperature records and mid-to-high latitude tree-ring density around the Northern Hemisphere, Volcanism and the Earth’s atmosphere, in: *Geoph. Monog. Series.*, 139, edited by: Robock, A. and Oppenheimer, C., 239–254, AGU Washington, D.C., 2003.
- Jury, M. R., McQueen, C., and Levey, K.: SOI and QBO Signals in the African Region, *Theor. Appl. Climatol.*, 50, 103–115, 1994.
- Kuleshov, Y., Chané Ming, F., Qi, L., Chouaibou, I., Hoareau, C., and Roux, F.: Tropical cyclone genesis in the Southern Hemisphere and its relationship with the ENSO, *Ann. Geophys.*, 27, 2523–2538, doi:10.5194/angeo-27-2523-2009, 2009.
- Lau, W. K. M. and Waliser, D. E. (Eds.): *Intraseasonal Variability of the Atmosphere-Ocean Climate System*, Springer-Verlag, Berlin, Germany, 474 pp., 2005.
- Lebouvier, M. and Frenot, Y.: “Conservation and Management in the French Sub Antarctic Islands and Surrounding Seas.” 23, *Papers and Proceedings of the Royal Society of Tasmania*, 141, 23–28, 2007.
- Liu, Y. and Lu, C.-H.: The influence of the 11-year sunspot cycle on the atmospheric circulation during winter, *Chinese J. Geophys.-Ch.*, 53, 354–364, 2010.
- Madden, R. A. and Julian, P. R.: Detection of a 40–50 day oscillation in the zonal wind in the tropical Pacific, *J. Atmos. Sci.*, 28, 702–708, 1971.
- Madden, R. A. and Julian, P. R.: Observations of the 40–50 day tropical oscillation: a review, *Mon. Weather Rev.*, 122, 814–837, 1994.
- McCormick, M. P. and Veiga, R. E.: SAGE II Measurements of Early Pinatubo Aerosols, *Geophys. Res. Lett.*, 19, 155–158, 1992.
- Meyers, G., McIntosh, P., Pigot, L., and Pook, M.: The years of El Niño, La Niña and interactions with the tropical Indian Ocean, *J. Climate*, 20, 2872–2880, 2007.
- Michalsky, J. J., Perez, R., Seals, R., and Ineichen, P.: Degradation of Solar Concentrator Performance in the Aftermath of Mount Pinatubo, *Sol. Energy*, 52, 205–213, 1994.
- Morioka, K., Tomoki, T., and Yamagata, T.: Climate variability in the southern Indian Ocean as revealed by self-organizing maps, *Clim. Dynam.*, 35, 1059–1072, doi:10.1007/s00382-010-0843-x, 2010.
- Percival, D. B. and Walden, A. T.: *Spectral Analysis for Physical Applications: Multitaper and Conventional Univariate Techniques*, Cambridge University Press, Cambridge, UK, 1993.
- Ramanathan, V.: The Greenhouse Theory of Climate Change: A Test by Inadvertent Global Experiment, *Science*, 240, 293–299, 1988.



- Robock, A. and Mao, J.: The Volcanic Signal in Surface Temperature Observations, *J. Climate*, 8, 1086–1103, 1995.
- Saji, N. H. and Yamagata, T.: Possible impacts of Indian Ocean Dipole Mode events on global climate, *Clim. Res.*, 25, 151–169, 2003.
- Saji, N. H., Goswami, B. N., Vinayachandran, P. N., and Yamagata, T.: A dipole mode in the tropical Indian Ocean, *Nature*, 401, 360–363, 1999.
- Schoeberl, M. R., Douglass, A. R., Newman, P. A., Lait, L. R., Lary, D., Waters, J., Livesey, N., Froidevaux, L., Lambert, A., Read, W., Filipiak, M. J., and Pumphrey, H. C.: QBO and annual cycle variations in tropical lower stratosphere trace gases from HALOE and Aura MLS Observations, *J. Geophys. Res.*, 113, D05301, doi:10.1029/2007JD008678, 2008.
- Shepherd, T. G.: Atmospheric circulation as a source of uncertainty in climate change projections, *Nature Geoscience*, 7, 703–708, 2014.
- Soden, B. J., Jackson, D. L., Ramaswamy, V., Schwarzkopf, D., and Huang, X.: The radiative signature of upper tropospheric moistening, *Science*, 310, 841–844, 2005.
- Stowe, L. L., Carey, R. M., and Pellegrino, P. P.: Monitoring the Mt. Pinatubo Aerosol Layer with NOAA-11 AVHRR Data, *Geophys. Res. Lett.*, 14, 159–162, 1992.
- Takayabu, Y. N., Iguchi, T., Kachi, M., Shibata, A., and Kanzawa, H.: Abrupt termination of the 1997–98 El Niño in response to a Madden–Julian oscillation, *Nature*, 402, 279–282, 1999.
- Thomas, M. A., Giorgetta, M. A., Timmreck, C., Graf, H.-F., and Stenchikov, G.: Simulation of the climate impact of Mt. Pinatubo eruption using ECHAM5 – Part 2: Sensitivity to the phase of the QBO and ENSO, *Atmos. Chem. Phys.*, 9, 3001–3009, doi:10.5194/acp-9-3001-2009, 2009.
- Timmreck, C. and Graf, H.-F.: The initial dispersal and radiative forcing of a Northern Hemisphere mid-latitude super volcano: a model study, *Atmos. Chem. Phys.*, 6, 35–49, doi:10.5194/acp-6-35-2006, 2006.
- Trenberth, K. E. and Dai, A.: Effects of Mount Pinatubo volcanic eruption on the hydrological cycle as an analog of geoengineering, *Geophys. Res. Lett.*, 34, L15702, doi:10.1029/2007GL030524, 2007.
- Trenberth, K. E. and Smith, L.: The mass of the atmosphere: a constraint on global analyses, *J. Climate*, 18, 864–875, 2005.
- Trenberth, K. E. and Stepaniak, D. P.: The flow of energy through the Earth’s climate system, *Q. J. Roy Meteor. Soc.*, 130, 2677–2701, 2004.
- Verosub, K. L. and Lippman, J.: Global Impacts of the 1600 Eruption of Peru’s Huaynaputina Volcano, *Eos Transactions, American Geophysical Union*, 89, 141–142, doi:10.1029/2008EO150001, 2008.
- Webster, P. J., Moore, A. M., Loschnigg, J. P., and Leben, R. R.: Coupled oceanic-atmospheric dynamics in the Indian Ocean during 1997–98, *Nature*, 401, 356–360, 1999.
- Wheeler, M. and Hendon, H.: An All-Season Real-Time Multivariate MJO Index: Development of an Index for Monitoring and Prediction, *Mon. Weather Rev.*, 132, 1917–1932, 2004.
- Yamagata, T., Behera, S. K., Rao, S. A., Guan, Z., Ashok, K., and Saji, H. N.: The Indian Ocean Dipole: a physical entity, *CLIVAR Exchanges*, 24, 15–18, 20–22, 2002.
- Yamagata, T., Behera, S. K., Rao, S. A., Guan, Z., Ashok, K., and Saji, H. N.: Comments on “Dipoles, temperature gradient, and tropical climate anomalies”, *B. Am. Meteorol. Soc.*, 84, 1418–1422, 2003.
- Yamagata, T., Behera, S. K., Luo, J.-J., Masson, S., Jury, M., and Rao, S. A.: Coupled ocean-atmosphere variability in the tropical Indian Ocean. *Earth Climate: The Ocean-Atmosphere Interaction*, *Geophys. Monogr., Amer. Geophys. Union*, 147, 189–212, 2004.
- Yin, X. G., Gruber, A., and Arkin, P.: Comparison of the GPCP and CMAP merged gauge-satellite monthly precipitation products for the period 1979–2001, *J. Hydrometeorol.*, 5, 1207–1222, 2004.
- Yuan, Y. and Li, C.: Decadal variability of the IOD-ENSO Relationship, *Chinese Science Bulletin*, 53, 1745–1752, 2008.
- Zhang, C.: Madden-Julian Oscillation, *Rev. Geophys.*, 43, RG2003, doi:10.1029/2004RG000158, 2005.